



ORIGINAL PAPER

ANALYSIS OF GNSS TIME SERIES NOISE CHARACTERISTICS AND DETECTION OF STATION VELOCITY OUTLIERS BASED ON IMPROVED BIC AND U-TEST

Ziyu WANG ¹⁾, Wei Jin ²⁾ and Xiaoxing HE ²⁾, *¹⁾ Xuzhou Surveying and Mapping Research Institute Co. Ltd, Xuzhou 221000, China²⁾ School of Civil and Surveying & Mapping Engineering, Jiangxi University of Science and Technology, Ganzhou, 341000, China

*Corresponding author's e-mail: xxh@jxust.edu.cn

ARTICLE INFO

Article history:

Received 20 August 2025

Accepted 21 December 2025

Available online 13 January 2026

13

Keywords:

GNSS Time Series

BIC_{tp}

Station Velocity Estimation

Noise Model

Anniversary Analysis

ABSTRACT

The presence of colored noise in GNSS coordinate time series can affect the accurate estimation of station velocity and velocity uncertainty. Accurate noise model identification is crucial for obtaining reliable and high-precision velocity estimates and their true confidence intervals. To address this, accurate noise model identification is critical for high-precision velocity estimates. The study selected 37 GNSS coordinate time series on the West Coast of the United States from 1999 to 2023, and we adopt a novel Bayesian Information Criterion with temporal prioritization (*BIC_{tp}*), extending the standard *BIC* by incorporating temporal factors to detect colored noise in GNSS coordinate time series, and compares it with *BIC* and the Akaike Information Criterion (*AIC*). The results show that *BIC_{tp}* effectively identifies distinct noise profiles, with the north (N) and east (E) components dominated by flicker noise plus random walk plus white noise (FNRWWN) and the up (U) component by power-law plus white noise (PLWN). Subsequently, the Mann-Whitney U-test and error propagation analysis assess the impact of these noise models on station velocity and annual amplitudes. Mean station velocity is significantly positive (0.07–0.20 mm/yr, 95 % confidence interval) with no outliers in velocity uncertainty. The U-test indicates that 70.3 % and 86.5 % of annual displacement amplitudes in the N and E components, respectively, are below 1.0 mm, suggesting stable horizontal motion, while vertical (U) displacements show greater annual variations. Non-parametric testing enhances the detection of anomalous velocity and periodic terms, improving velocity and amplitude estimate accuracy by identifying data processing errors.

1. INTRODUCTION

GNSS coordinate time series provide critical data for determining station velocity fields and its uncertainties, enabling applications in geodetic and geodynamic research (Zhou et al., 2025; Zhu et al., 2023; Hu et al., 2025; Huang et al., 2025). These applications include establishing coordinate reference frames (Benciolini et al., 2008; Nicolini and Caporali, 2018), monitoring crustal deformation and block motion (Mendoza et al., 2015; Poyraz et al., 2019), assessing structural deformation (Yu et al., 2025), monitoring landslide (Huang et al., 2023), measuring ground subsidence (Cina and Piras, 2015; Shu et al., 2023), and quantifying sea level changes (Sun et al., 2024; Zhou et al., 2022). Advances in earth sciences and engineering have increased the demand for high-precision GNSS velocity estimates, particularly for studies of global and regional crustal deformation requiring detailed three-dimensional tectonic characteristics and for maintaining modern geodetic reference frames, which demand velocity accuracies of 0.1 mm/yr (Dmitrieva et al., 2015; Altamimi et al., 2016; Özdemir and Karşlıoğlu, 2019; Glaser et al., 2020).

Periodic signals in GNSS time series, including annual and semi-annual, as well as draconitic cycles, significantly influence velocity estimation (He et al., 2017; Amiri-Simkooei, 2013; Springer et al., 2019). Unmodeled or inaccurately estimated seasonal signals can bias velocity estimates, as their amplitudes vary over time (Klos et al., 2018; Hu et al., 2022). Incorporating time-varying periodic signals into time series models is thus essential to enhance the accuracy of reference station velocity fields. GNSS time series contain not only white noise (WN) but also colored noise, such as flicker noise (FN), random walk (RW), and Generalized Gaussian Markov (GGM) noise, which complicates velocity estimation (Williams, 2003; Amiri-Simkooei et al., 2007). Huang et al. (2025) investigated the accurate estimation of noise models in GNSS coordinate time series in the presence of Offsets and their impact on velocity estimation. Through simulations and real data, they demonstrated the necessity of jointly estimating offsets, trends, periodic signals, and noise models (such as FNWN). Wang et al. (2025) proposed a novel dual-denoising method (COA-VMPE-WD) and evaluated noise models including FNWN, FNRWWN, and PLWN, the

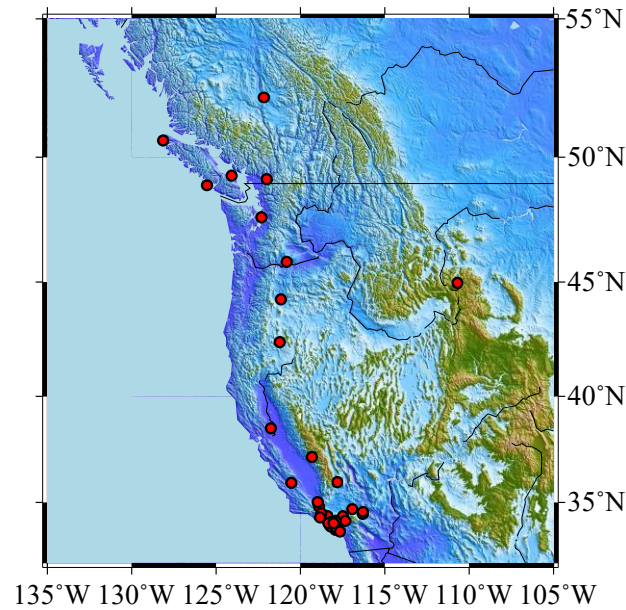


Fig. 1 Spatial distribution of the analyzed sites.

method effectively suppresses complex noise in time series and alters the noise model, thereby providing insights for improving the accuracy of velocity estimation. Spectral analysis of GNSS time series in Australian plate revealed negative power spectral indices, confirming FN prevalence (Jiang and Zhou, 2015). However, GGM noise is often overlooked due to conservative velocity uncertainty estimates. Increasing noise model complexity introduces additional parameters, leading to higher likelihood estimates and potential bias in traditional maximum likelihood estimation (MLE) methods (Langbein, 2008). To address overfitting, the Akaike Information Criterion (AIC) and Bayesian Information Criterion (BIC) incorporate penalty terms (Akaike, 1974; Schwarz, 1978). Limited sample sizes in long-period GNSS time series further challenge accurate noise model estimation, prompting enhancements like BIC constants (Schwarz, 1978). Regional studies, such as Jin et al. (2020), identified FNWN in the east (E), north (N), and up (U) components of coastal China GNSS stations, with a mix of WN, GGM, and RW in the N component, increasing velocity mean square error by 5–10 times compared to a single WN model. Zhang et al. (1997) found that WN and FNWN models yield equivalent velocity estimates at a 95 % confidence level, suggesting the need for robust statistical tests like the Mann-Whitney U-test to detect time series anomalies (Ren et al., 2022). Inappropriate noise models can bias velocity uncertainty estimates, distort regional velocity fields, and compromise high-precision geodynamic applications (Wang et al., 2012; Bock and Melgar, 2016; He et al., 2017; Langbein, 2012; Montillet et al., 2019). These diverse and regionally variable noise characteristics necessitate advanced modeling approaches.

To address these challenges, this study proposes a Bayesian Information Criterion with temporal prioritization (BIC_{tp}), which extends BIC by incorporating temporal factors to improve colored noise detection in GNSS time series (Zhang et al., 2025). BIC_{tp} is compared with AIC and standard BIC across four prevalent noise models: flicker noise plus white noise (FNWN), power-law plus white noise (PLWN), generalized Gaussian Markov plus white noise (GGMWN), and flicker noise plus random walk plus white noise (FNRWWN). Using the FNWN model, the Mann-Whitney U-test validates GNSS station velocity reliability, and the impact of different noise models on velocity and annual amplitude estimation is assessed. This approach aims to enhance the precision of GNSS velocity estimates, supporting high-accuracy geodynamic research.

2. DATA AND METHODS

2.1. DATA SOURCES

To explore the improvement of Bayesian information estimation for GNSS station coordinate temporal colored noise, we utilize 24 years of coordinate time series from 37 GNSS reference station networks on the West Coast of the United States (with access of http://garner.ucsd.edu/pub/measuresESESES_products). We use U-test and velocity error theory to explore the characteristics of GNSS station coordinate temporal noise models. The station distribution map is shown in Figure 1, and the time series of BGIS station coordinates in different components is shown in Figure 2.

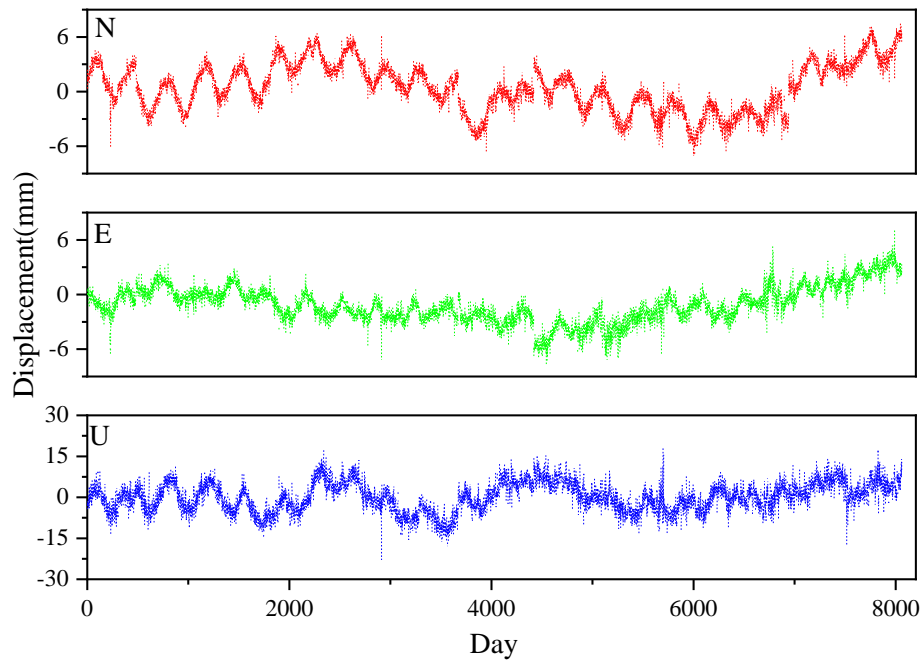


Fig. 2 An example of GNSS coordinate time series (BGIS Site).

2.2. AKAIKE INFORMATION CRITERIA

He et al. (2017) found that Akaike Information Criteria (*AIC*) has certain limitations. The principle of *AIC* is :

$$AIC = 2k - 2 \ln L \quad (1)$$

k is the number of unknown parameters in the noise model combination ; L is the maximum likelihood function value likelihood function in the model; When selecting the best model, choose the one with the smallest *AIC* value as the optimal noise model.

2.3. BAYESIAN INFORMATION CRITERION

The Bayesian Information Criterion (*BIC*) needs to introduce a penalty term to compensate for overfitting caused by too many unknown parameters (Nikolaidis, 2002; He et al., 2019). However, the *BIC* takes the sample size into account, resulting in a larger penalty term. In cases with a large sample size, it effectively prevents excessively high model complexity due to overly precise model fitting. The principle of the *BIC* is as follows (Sun et al., 2023):

$$BIC = k \ln(n) - 2 \ln(L) \quad (2)$$

n is the sample size; k is the number of unknown parameters in the noise model combination; L is the maximum likelihood function value and likelihood function in the model. When selecting the best model, choose the minimum *BIC* value as the optimal noise model.

For long time series, *AIC* and *BIC* can better identify additional parameters in the noise model and

has the greatest impact on GGMWN. Thus, we establish noise model estimation criterion *BIC_{tp}* between *BIC* by introducing 2π factor. The principle is as follows (He et al., 2017) :

$$BIC_{tp} = -2 \log(L) + \log\left(\frac{n}{2\pi}\right)v \quad (3)$$

L is the likelihood function, n is the length of the time series, v represents the number of model parameters, $\log(L)$ represents the likelihood function of the maximum likelihood function value in the noise model, and the smaller the value of *BIC_{tp}*, the higher the accuracy of parameter estimation.

2.4. U-TEST MATHEMATICAL MODEL

Gross error is commonly present in long-term GNSS coordinate time series (Wang et al., 2016). To improve the reliability of experimental results, it is necessary to further detect and eliminate abnormal station data. Zhang et al. (1997) indicates that at the significance level ($\alpha=0.05$), the station velocity estimated by the pure white noise model is equal to the estimated value by the FNWN combined noise model. Therefore, the velocity residuals of the two are used as test variables. If the expected value of the velocity residuals is 0, it indicates that the data at the station is normal; Otherwise, it indicates significant gross errors in the data from the station. Different combinations of noise models may alter the estimated velocities and their uncertainties. To systematically analyze this impact and determine whether the velocities derived from different noise models are statistically significantly different, we introduced the U-test, the difference between the station velocity estimated by

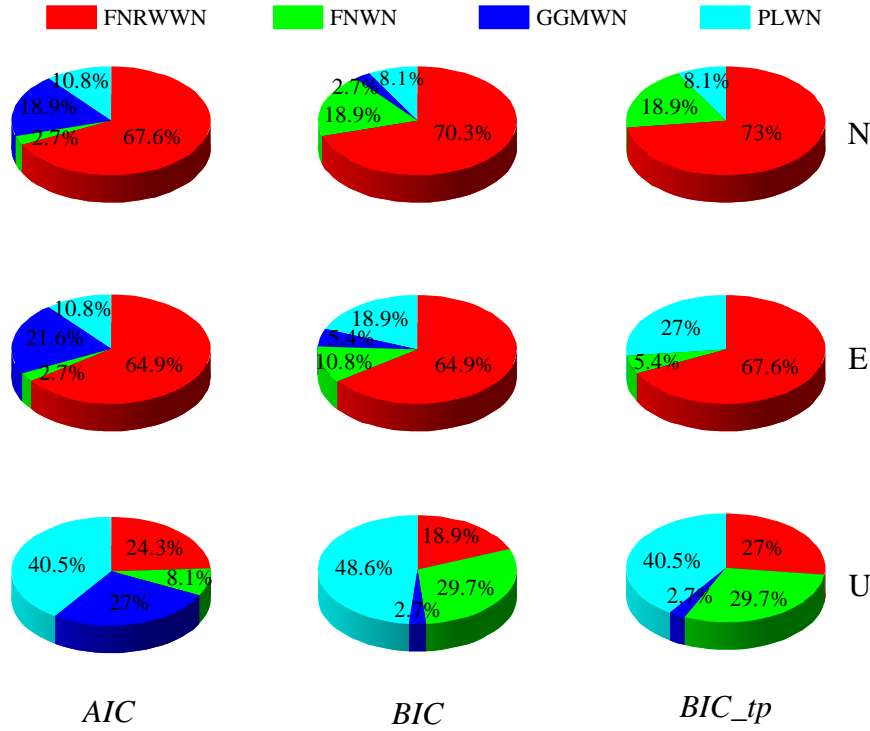


Fig. 3 Statistical distribution of noise models in different components.

pure white noise at each station and the estimated value of the FNWN combined noise model is used as the test variable for U-test. The principle is as follows (Sun et al., 2023) :

$$|\omega_i| = \frac{|dV_i|}{\sigma_0 \sqrt{(Q_{dVdV})_{ii}}} \quad (4)$$

Where V_i is the velocity uncertainty, dV_i is the integral of the velocity, $\sigma_0 \sqrt{(Q_{dVdV})_{ii}}$ is the standard deviation of the velocity, and ω_i is the standard statistic (Sun et al., 2023).

2.5. MATHEMATICAL MODEL FOR STATION VELOCITY AND VELOCITY UNCERTAINTY

Bos et al. (2013) and Klos et al. (2014) adopt linear regression fitting method, which is widely used in estimating GNSS station velocity. The mathematical model of station velocity is (He et al., 2019):

$$m_{v_v} \approx \pm \frac{\sqrt{\frac{A_{PLv}^2}{\Delta T_{vv}^2} \cdot \frac{\tau_{vv}(3-\kappa_{vv}) \cdot \tau_{vv}(4-\kappa_{vv}) \cdot (N_{vv}-1)^{\kappa_{vv}-3}}{[\tau_{vv}(2-\frac{\kappa_{vv}}{2})]^2}}}{\Delta T_{vv}^2} \quad (5)$$

N_{vv} is the length of the observed time series, κ_{vv} is the estimated spectral index; ΔT_{vv} is the sampling rate; A_{PLv} is the amplitude of noise; τ_{vv} is the gamma function.

According to equation (5), we use velocity variance δ to characterize the uncertainty of station velocity. As the length of the time series increases, the ratio of velocity uncertainty shows an upward trend

(Steinbock et al., 2016). The mathematical model of station velocity is (Sun et al., 2024):

$$\delta^2 = (m_{v_1} - \bar{m}_v)^2 + \frac{(m_{v_2} - \bar{m}_v)}{(n-1)} \quad (6)$$

\bar{m}_v is the average velocity value n is the number of observations. The larger δ , the greater the uncertainty; The smaller δ , the smaller the uncertainty.

3. RESULTS AND DISCUSSION

3.1. COMPARATIVE ANALYSIS OF ESTIMATION CRITERIA FOR DIFFERENT NOISE MODELS

To compare and analyze the impact of different noise model estimation criteria on the coordinate time series of GNSS stations, *AIC*, *BIC* and *BIC_{tp}* were used to estimate the noise in the coordinate time series. The statistical results of the optimal noise models in the N, E, and U components are shown in Figure 3.

According to Figure 3, in the N component of *AIC* and *BIC* noise estimation, the main models are FNRWWN (about 67.6 %, 70.3 %), GGMWN (about 18.9 %, 2.7 %), and PLWN (about 10.8 %, 8.1 %); The main manifestations in the E component are the FNRWWN model (approximately 64.9 %, 64.9 %), GGMWN model (approximately 21.6 %, 5.4 %), and PLWN model (approximately 10.8 %, 18.9 %); In the U component, it mainly manifests as PLWN model (about 40.5 %, 48.6 %), GGMWN model (about 27 %, 2.7 %), and FNRWWN model (about 24.3 %, 18.9 %). In *BIC_{tp}* noise mode estimation, the N component is mainly represented by FNRWWN model (about 73 %), FNWN model (about 18.9 %), and PLWN model (about 8.1 %); In the E component, the main

Table 1 Values of extreme station velocity in different components and models (Unit: mm/yr).

Component	Value	FNRWWN	FNWN	GGMWN	PLWN
N	Max	1.51	1.87	1.69	1.67
	Min	-2.14	-2.08	-2.10	-2.14
	Mean	0.12	0.07	0.10	0.11
E	Max	0.77	0.63	0.64	0.65
	Min	-0.45	-0.67	-0.85	-0.96
	Mean	0.05	-0.02	-0.03	-0.03
U	Max	1.38	1.41	1.40	1.44
	Min	-0.47	-0.27	-0.29	-0.27
	Mean	0.19	0.21	0.18	0.20

manifestations are FNRWWN model (about 67.6 %), PLWN model (about 27 %), and partially FNWN model (about 5.4 %). *BIC_{tp}* didn't detect the GGMWN model on the N and E components, but hidden RW noise was detected; In the U component, it mainly manifests as PLWN model, FNWN model (about 29.7 %), and FNRWWN model (about 27 %). Compared to *AIC* and *BIC*, the *BIC_{tp}* estimation criterion demonstrates greater sensitivity to the FNRWWN model. In the three components analysis, *BIC_{tp}* increased the identification rates of the FNRWWN model by 5.4 % (N), 2.7 % (E), and 2.7 % (U), respectively, significantly surpassing the original proportions obtained with the *AIC*. Notably, for U component, *BIC_{tp}* achieved a substantial improvement of 8.1 % in identification rate compared to *BIC*, highlighting the significance of this enhancement. In summary, we know that noise models differ significantly the horizontal and vertical components, demonstrating that GNSS time series exhibit diverse, multi-component noise characteristics. Therefore, accurately characterizing this complex noise, particularly in the vertical component, requires a robust estimation criterion. The *BIC_{tp}* criterion demonstrates superior capability in this regard, as it more effectively identifies the composite noise features (FNRWWN) that characterize complex vertical time series.

3.2. ANALYSIS OF THE IMPACT OF COLORED NOISE ON STATION VELOCITY DURING U-TEST DETECTION

3.2.1. THE IMPACT OF DIFFERENT NOISE MODELS ON STATION VELOCITY

Further exploring the impact of noise models on station velocity and its uncertainty, the optimal noise model estimates the station velocity for different components of GNSS stations as shown in Figure 4, the unit of velocity in the figure is millimeter per year (abbreviated as mm/yr), the extreme velocity values of all GNSS stations under different components and models are shown in Table 1. Based on the FNRWWN noise model, the station velocities were subtracted from other noise estimates and subjected to independent sample Mann Whitney U-test with a significance level of 0.05.

According to Figure 4 and Table 1, the combined model comparative analysis of GNSS coordinate time series noise characteristics (FNRWWN, FNWN, GGMWN, PLWN) shows systematic differences in the N, E, and U components among the noise models. The maximum station velocity of the U component is 1.38 mm/yr -1.44 mm/yr, with a significantly positive mean (0.18 mm/yr ~0.21 mm/yr), but the maximum value of PLWN is slightly higher (Max=1.44 mm/yr), which may have a slight disadvantage in elevation positioning.

The fluctuation range on the N component (- 2.14 mm/yr ~1.87 mm/yr) is significantly larger than that on the E component (-0.96 mm/yr ~0.65 mm/yr), which may be related to the anisotropy of regional tectonic movements.

In terms of model performance, the average velocity of the N component in the FNWN model (0.07 mm/yr) is closest to the theoretically expected zero. In the E component, the average velocity estimated by all models is close to zero, ranging from -0.03 mm/yr to 0.05mm/yr. It is worth noting that the average values of FNWN and GGMWN models are negative on the E component.

3.2.2. STATION VELOCITY ANOMALY DETECTION BASED ON U-TEST

To improve the reliability of experimental results, further detection and removal of abnormal station data were carried out. Independent U-test was performed on the station velocities estimated by the FNWN combined noise model for each station component, with a significance level set at 0.05. After U-test detection, the results showed that the FNWN combined noise model with N, E, and U components estimated the same station velocity distribution as the WN single noise model, indicating that there was no significant difference in statistics. After testing two independent samples through U-test, interval estimation was performed on the velocity residuals. The statistical results of the velocity residuals for each component are shown in Figure 5.

The statistical results of the velocity difference of the three components in U-text in Figure 5. At a significance level of 0.05, the confidence intervals for the N component velocity difference are [- 0.29 mm/yr, 0.21 mm/yr], the E component velocity difference is [-0.11 mm/yr, 0.10 mm/yr], and the U

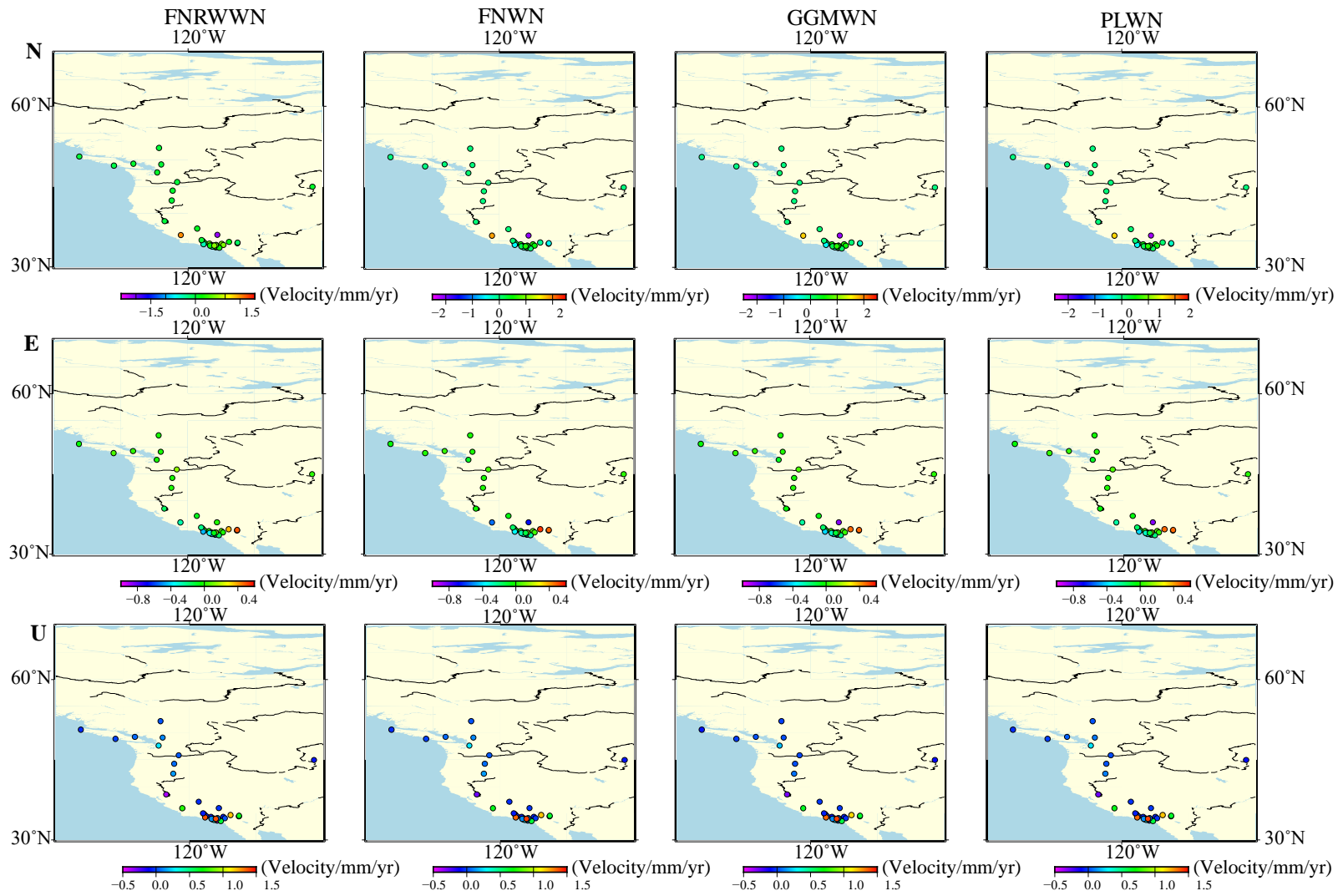


Fig. 4 Velocity distribution of stations with different noise models in three components.

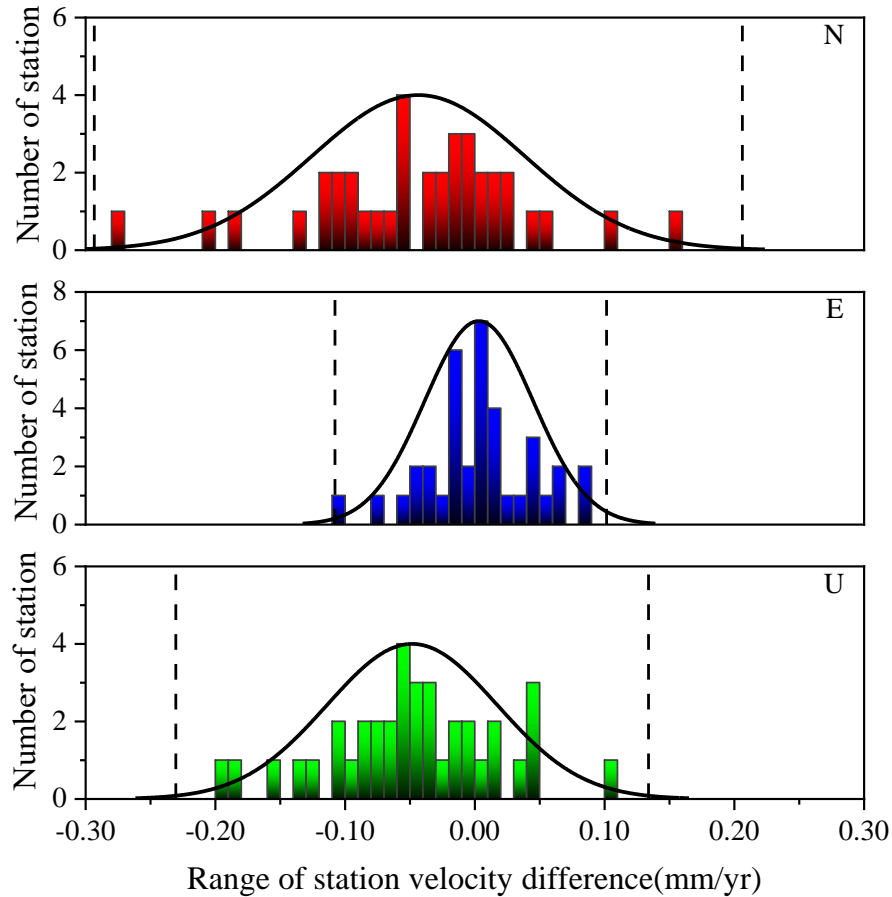


Fig. 5 Statistical results of velocity difference between N, E, and U components after U-text.

Table 2 Extreme value of velocity difference between different noise model stations (Unit: mm/yr).

Model \ Value	FNRWWN-FNWN			GGMWN-FNWN			PLWN-FNWN		
	N	E	U	N	E	U	N	E	U
Max	0.48	0.34	0.59	0.46	0.29	0.15	0.49	0.33	0.08
Min	0	0	0	0	0	0	0	0	0
Mean	0.06	-0.01	-0.01	0.03	-0.01	-0.02	0.03	-0.01	-0.01

component velocity difference is [-0.23 mm/yr, 0.13 mm/yr]. The velocity residuals of each station fall within the confidence intervals, indicating that there are no significant gross errors in the selected station data and that the estimated station velocities are highly reliable. It also indicates that the presence of FN has no significant impact on velocity estimation. Further statistical analysis was conducted on the estimated station velocity values, with FNWN as the benchmark. The extreme values of station velocity differences for different noise models are shown in Table 2.

According to Table 2, the maximum difference in station velocity for different noise models with N components is 0.49 mm/yr, the minimum is 0, and the average is less than 0.06 mm/yr; The maximum difference in station velocity between different noise models with E component is 0.34 mm/yr, the minimum is 0, and the average is about 0.01 mm/yr; The maximum difference in station velocity between different noise models with U component is

0.59 mm/yr, the minimum is 0, and the average is less than -0.01 mm/yr. In summary, the minimum difference in station velocity between different noise models on different components is 0, and the difference between FNRWWN and FNWN is relatively large, further indicating that there are certain differences in the impact of different noise models on GNSS station velocity, and the impact of RW on station velocity cannot be ignored.

3.3. THE IMPACT OF COLORED NOISE ON GNSS STATION VELOCITY UNCERTAINTY

3.3.1. ANALYSIS OF GNSS STATION VELOCITY UNCERTAINTY WITH COLORED NOISE

We further analyze the impact of colored noise on station velocity uncertainty. The uncertainty of station velocity is shown in Figure 6, the extreme velocity uncertainty values of GNSS stations under different components and models are shown in Table 3.

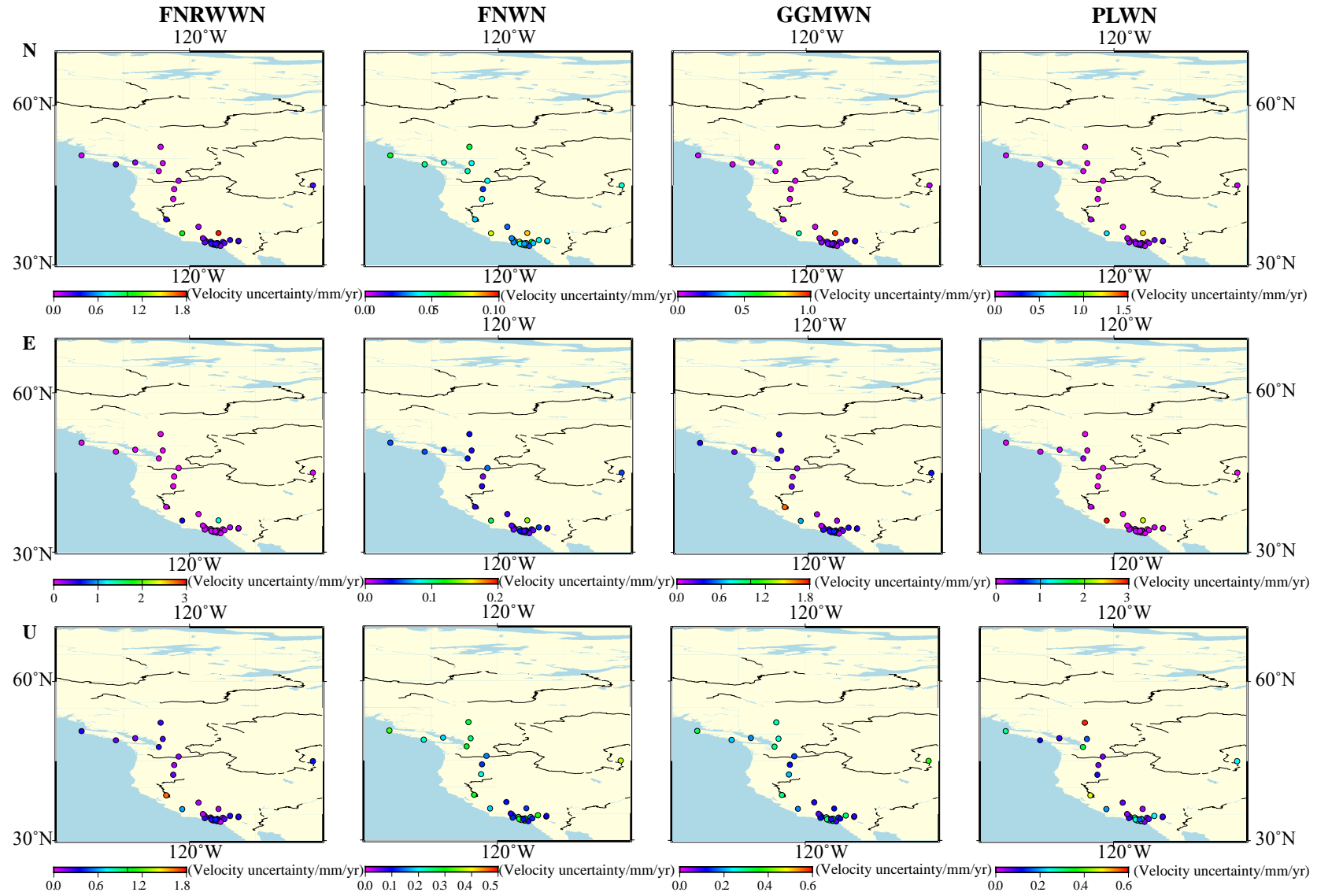


Fig. 6 Velocity uncertainty distribution of stations with different noise models in three components.

Table 3 Values of extreme station velocity uncertainty in different components and models (Unit: mm/yr).

Component	Value	FNRWWN	FNWN	GGMWN	PLWN
N	Max	1.77	0.09	0.96	1.25
	Min	0.04	0.02	0.01	0.02
	Mean	0.32	0.04	0.12	0.17
E	Max	2.91	0.14	1.73	2.98
	Min	0.02	0.02	0.01	0.01
	Mean	0.36	0.04	0.15	0.24
U	Max	1.66	0.38	0.52	0.92
	Min	0.08	0.08	0.04	0.04
	Mean	0.33	0.20	0.13	0.21

According to Table 3, different FNRWWN models exhibit the larger fluctuation range in all components (N: 1.77 mm/yr, E: 2.91 mm/yr, U: 1.66 mm/yr), while the FNWN model shows the best stability (range less than 0.38 mm/yr in all components). The noise amplitude in the E component is significantly greater than that U component, with the maximum fluctuation in the E component reaching 2.98 mm/yr (PLWN), which may be related to the directional characteristics of the multipath effect of the receiver antenna. The FNWN model has the smaller mean in all components (N: 0.04 mm/yr, E: 0.04 mm/yr, U: 0.20 mm/yr), indicating its best performance in eliminating systematic bias.

From Figure 6, there are significant differences in velocity uncertainty in the N, E, and U component s under different noise models, with velocity uncertainty in the U component generally higher than in the N and E components. The velocity uncertainty of the FNWN noise model station in the U component is 2.10-10.21 and 1.81-10.50 times that of the N and E components, respectively. The study compares and analyzes the optimal noise model FNRWWN with the FNWN noise model. The results show that the velocity uncertainty of FNRWWN in the N, E, and U component s is 19.21, 13.72, and 10.51 times that of the FNWN model, respectively. The velocity uncertainties estimated by CHWK, MDMT, and WILL stations under FNRWWN and FNWN noise models are similar, with ratios of approximately 1 in the N, E, and U components. In summary, the uncertainty of station velocity estimated based on the combined noise assumption of FNWN is too optimistic in the E component. The noise model exhibits diversity in spatial distribution. RW has a significant impact on the estimation of velocity uncertainty, and is reflected in the N, E, and U components. The influence of RW on velocity and its uncertainty cannot be ignored.

3.4. ANALYSIS OF U-TEST ON THE ANNUAL TERM BASED DIFFERENT COLORED NOISES

To improve the reliability of experimental results, further U-test analysis was conducted on the annual term of GNSS stations. The distribution of annual terms in different components for different noise models is shown in Figure 7~ Figure 9. Detect

and eliminate the annual amplitude of GNSS stations, introduce independent sample Mann Whitney U-test, and set the significance level to 0.05. After testing two independent samples through U-text, the annual amplitude statistics of each component are shown in Figure 10.

From Figures 7~9, the amplitude periodicity of the annual term is significant for different components and models. The amplitude of the U component with different noise models is higher than that of the N and E components. In the E component, the amplitude displacement of the PLWN noise model is the largest about 5.51 mm/yr), and its noise model amplitude displacement is about 2.53 times that of the N component noise model amplitude displacement; In the U component, the FNRWWN noise model has the largest amplitude displacement (about 5.51 mm/yr), and its noise model amplitude displacement is about 5.80 times that of the N component noise model, indicating that the annual motion of the station is greatly affected by the noise model in the U component. Perform U-test analysis on the annual term of GNSS stations, and verify the amplitude of the annual term in different components as shown in Figure 10.

According to Figure 10, after detection by the U- text method, at a significance level of 0.05, the amplitude of the three components follows a normal distribution, indicating that there is no abnormality in the amplitude. The confidence intervals for the amplitude of the N component annual term are [- 0.26 mm, 0.23 mm], the confidence intervals for the amplitude of the E component annual term are [- 0.36 mm, 0.47 mm], and the confidence intervals for the amplitude of the U component annual term are [-1.24 mm, 1.17 mm]. The annual term amplitudes of all stations fall within the confidence intervals, indicating that there is no significant gross error in the selected station data in the study, and the estimated annual term amplitudes are highly reliable.

4. CONCLUSIONS

The time-varying, noise model, tremor and other factors caused by geophysical effects are still the main reasons affecting the accurate acquisition of the velocity field and its uncertainty at the reference station. This study compared and analyzed the AIC,

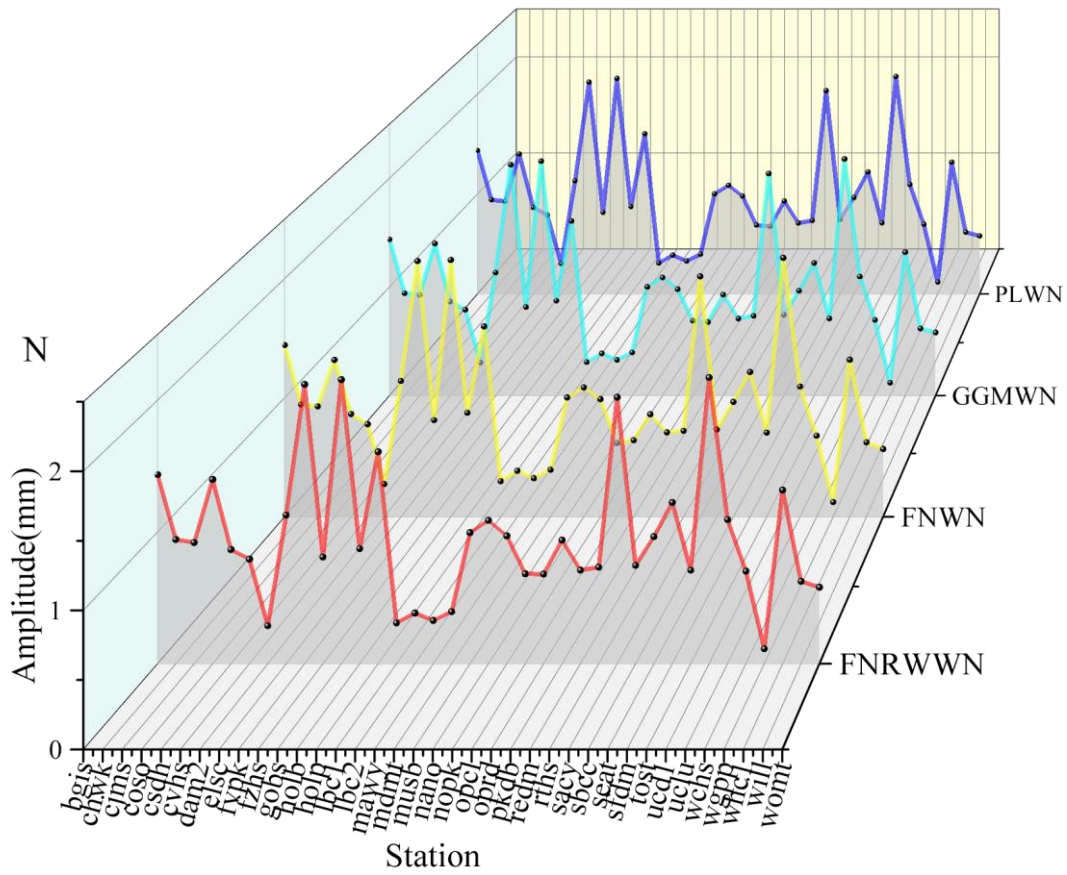


Fig. 7 Amplitude under different models on the N component.

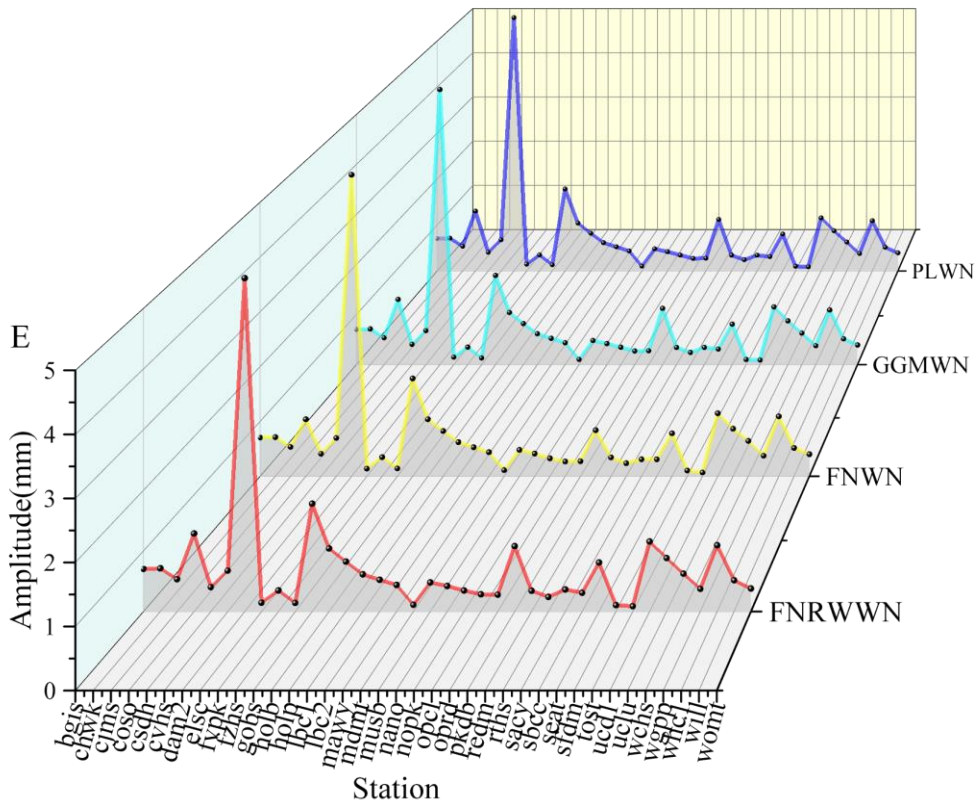


Fig. 8 Amplitude under different models on the E component.

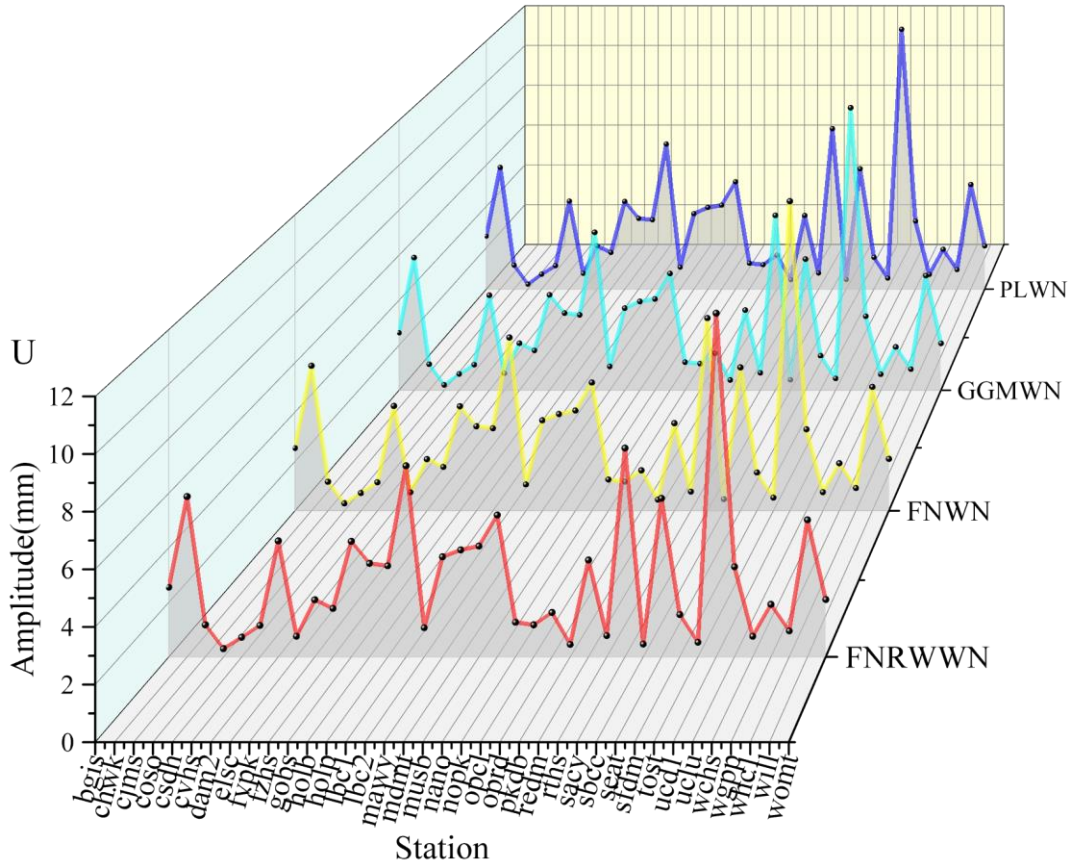


Fig. 9 Amplitude under different models on the U component.

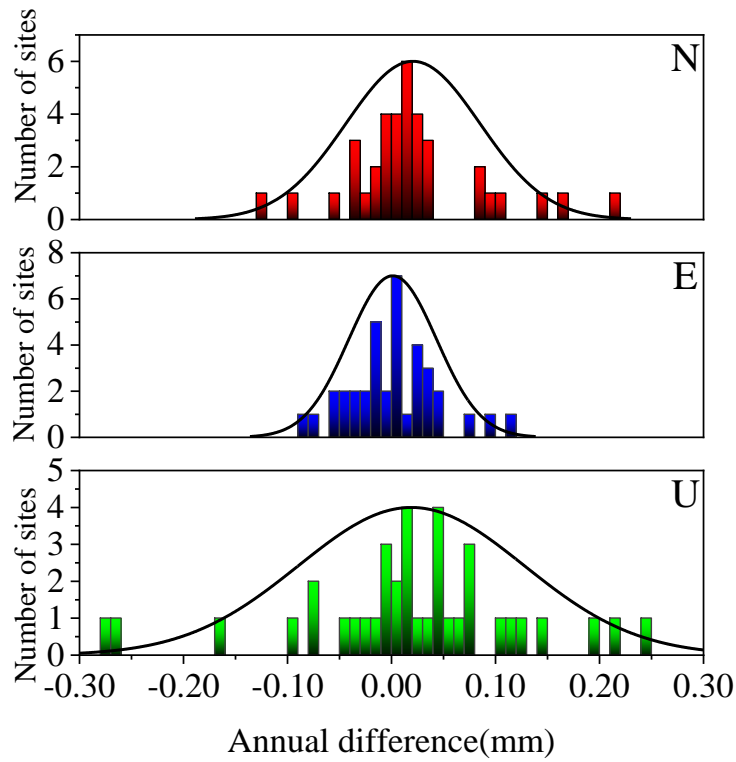


Fig. 10 Annual amplitude U-test for different components.

BIC, and *BIC_{tp}* noise model estimation criteria. Through different noise model estimation criteria, U-test and velocity error theory was introduced to analyze the impact of colored noise models on station velocity and velocity uncertainty estimation. Our conclusions were as follows:

1. The *BIC_{tp}* has significant advantages in identifying complex composite noise, such as FNRWWN. In the N and E components, the noise is predominantly characterized as FNRWWN, while in the U component, it is primarily PLWN. Compared to *AIC*, *BIC_{tp}* improves the identification rates of FNRWWN in the NEU components by 5.4 %, 2.7 %, and 2.7 %, respectively. Notably, for the U component, *BIC_{tp}* achieves an 8.1 % higher identification rate for FNRWWN compared to *BIC*, further validating its effectiveness in detecting complex vertical noise.
2. The station velocity and velocity uncertainty detected by U-text show a normal distribution, and there are significant differences in the impact of different noise models on GNSS station velocity estimation. On the N component, velocity is sensitive to model selection, and the FNWN model is closest to the theoretical zero value average velocity (0.07 mm/yr). However, the velocity difference between FNRWWN and FNWN models is significant, and the impact of RW noise on velocity uncertainty cannot be ignored. In the E component, the average velocity of FNWN and GGMWN models is negative, while in the U component, the velocities of each model are relatively close.
3. The annual motion of GNSS stations has a more significant impact on the U component. Approximately 70.3 % and 86.5 % of the annual amplitude displacements for the N and E components are less than 1.0mm, respectively, indicating relatively stable station motion. The U component stations mainly exhibit FNRWWN and PLWN noise model characteristics, and further research is needed to consider the RW effects that may be caused by external environment of the stations or undetected non- structural movements such as Offset.

The low-frequency RW noise present in the reference station may lead to an overestimation of the velocity field of the reference station. Therefore, accurately detecting RW noise is of great significance for obtaining high-precision station velocity parameters. Dmitrieva et al. (2015) proposed an observation network noise model estimation method based on stack averaging, which can detect small-scale random walk noise; In the future, the rigor of the noise model characteristics of regional benchmark stations, especially when there are significant differences in noise characteristics between different stations, needs to be further verified. Therefore, the estimation method of noise models needs further improvement and research.

ACKNOWLEDGMENTS

This work was sponsored by Outstanding Youth Fund of Jiangxi Natural Science Foundation (20252BAC220015). Jiangxi Province 2025 Graduate Innovation Special Fund Project (YC2025-S582).

REFERENCES

- Altamimi, Z., Rebischung, P., Métivier, L. and Collilieux, X.: 2016, ITRF2014: A new release of the International Terrestrial Reference Frame modeling nonlinear station motions. *J. Geophys. Res., Solid Earth*, 121, 6109–6131. DOI: 10.1002/2016JB013098
- Amiri-Simkooei, A.R., Tiberius, C.C. and Teunissen, P.J.: 2007, Assessment of noise in GPS coordinate time series: methodology and results. *J. Geophys. Res., Solid Earth*, 112, B7. DOI: 10.1029/2006JB004913
- Amiri-Simkooei, A.R.: 2013, On the nature of GPS draconitic year periodic pattern in multivariate position time series. *J. Geophys. Res., Solid Earth*, 118, 5, 2500–2511. DOI: 10.1002/jgrb.50199
- Benciolini, B., Biagi, L., Crespi, M., Manzano, A.M. and Roggero, M.: 2008, Reference frames for GNSS positioning services: Some problems and proposed solutions. *J. Appl. Geod.*, 2, 1, 53–68. DOI: 10.1515/JAG.2008.006
- Bock, Y. and Melgar, D.: 2016, Physical applications of GPS geodesy: A review. *Rep. Prog. Phys.*, 79, 10, 106801. DOI: 10.1088/0034-4885/79/10/106801
- Bos, M.S., Fernandes, R.M.S., Williams, S.D.P. and Bastos, L.: 2013, Fast error analysis of continuous GNSS observations with missing data. *J. Geod.*, 87, 4, 351–360. DOI: 10.1007/s00190-012-0605-0
- Cina, A. and Piras, M.: 2015, Performance of low-cost GNSS receiver for landslides monitoring: Test and results. *Geomat. Nat. Hazards Risk*, 6, 5-7, 497–514. DOI: 10.1080/19475705.2014.889046
- Dmitrieva, K., Segall, P. and DeMets, C.: 2015, Network-based estimation of time-dependent noise in GPS position time series. *J. Geod.*, 89, 6, 591–606. DOI: 10.1007/s00190-015-0801-9
- Glaser, S., Michalak, G., Männel, B., König, R., Neumayer, K.H. and Schuh, H.: 2020, Reference system origin and scale realization within the future GNSS constellation “Kepler”. *J. Geod.*, 94, 12, 117. DOI: 10.1007/s00190-020-01441-0
- He, X., Montillet, J.P., Fernandes, R., Bos, M., Yu, K., Hua, X. and Jiang, W.: 2017, Review of current GPS methodologies for producing accurate time series and their error sources. *J. Geodyn.*, 106, 12–29. DOI: 10.1016/j.jog.2017.01.004
- He, X., Montillet, J.P., Hua, X., Yu, K., Jiang, W. and Zhou, F.: 2017, Noise analysis for environmental loading effect on GPS position time series. *Acta Geodyn. Geomater.*, 14, 1, 131–142. DOI: 10.13168/AGG.2016.0034
- Hu, S., Chen, K., Zhu, H., Xue, C., Wang, T., Yang, Z. and Zhao, Q.: 2022, A comprehensive analysis of environmental loading effects on vertical GPS time series in Yunnan, southwest China. *Remote Sens.*, 14, 12, 2741. DOI: 10.3390/rs14122741
- Huang, G., Du, S. and Wang, D.: 2023, GNSS techniques for real-time monitoring of landslides: A review. *Satell. Navig.*, 4, 1, 5. DOI: 10.1186/s43020-023-00095-5

- Huang, J., He, X., Hu, S. and Ming, F.: 2025, Impact of offsets on GNSS time series stochastic noise properties and velocity estimation. *Adv. Space Res.*, 75, 4, 3397–3413. DOI: 10.1016/j.asr.2024.12.016
- Jiang, W. and Zhou, X.: 2015, Effect of the span of Australian GPS coordinate time series in establishing an optimal noise model. *Sci. China Earth Sci.*, 58, 4, 523–539. DOI: 10.1007/s11430-014-4996-z
- Jin, B., Wang, H., Liu, Y., Deng, L. and Lyu, J.: 2020, Establishment and analysis of GNSS coordinate time series noise model for coastal tide stations in China. *J. Geod. Geodyn.*, 40, 5, 476–481. DOI: 10.14075/j.jgg.2020.05.007
- Klos, A., Bogusz, J., Figurski, M. and Kosek, W.: 2014, Uncertainties of geodetic velocities from permanent GPS observations: the Sudeten case study. *Acta Geodyn. Geomater.*, 11, 3, 201–209. DOI: 10.13168/AGG.2014.0005
- Klos, A., Olivares, G., Teferle, F.N., Hunegnaw, A. and Bogusz, J.: 2018, On the combined effect of periodic signals and colored noise on velocity uncertainties. *GPS Solut.*, 22, 1, 1. DOI: 10.1007/s10291-017-0674-x
- Langbein, J.: 2008, Noise in GPS displacement measurements from Southern California and Southern Nevada. *J. Geophys. Res., Solid Earth*, 113, B5. DOI: 10.1029/2007JB005247
- Langbein, J.: 2012, Estimating rate uncertainty with maximum likelihood: differences between power-law and flicker-random-walk models. *J. Geod.*, 86, 9, 775–783. DOI: 10.1007/s00190-012-0556-5
- Mendoza, L., Richter, A., Fritsche, M., Hormaechea, J.L., Perdomo, R. and Dietrich, R.: 2015, Block modeling of crustal deformation in Tierra del Fuego from GNSS velocities. *Tectonophysics*, 651, 58–65. DOI: 10.1016/j.tecto.2015.03.013
- Montillet, J.P. and Bos, M.S.: 2019, Conclusions and future challenges in geodetic time series analysis. In: *Geodetic Time Series Analysis in Earth Sciences*, Springer International Publishing, 419–422. DOI: 10.1007/978-3-030-21718-1_13
- Nicolini, L. and Caporali, A.: 2018, Investigation on reference frames and time systems in multi-GNSS. *Remote Sens.*, 10, 1, 80. DOI: 10.3390/rs10010080
- Nikolaidis, R.: 2002, Observation of geodetic and seismic deformation with the Global Positioning System. University of California, San Diego. <https://www.proquest.com/openview/367a8a2afabf8709955b5ed9c8ecee21/1?cbl=18750&diss=y&ppq-origsite=gscholar>
- Özdemir, S. and Karslıoğlu, M.O.: 2019, Soft clustering of GPS velocities from a homogeneous permanent network in Turkey. *J. Geod.*, 93, 8, 1171–1195. DOI: 10.1007/s00190-019-01235-z
- Poyraz, F.A.T.İ.H., Hastaoğlu, K.O., Kocbulut, F.İ.K.R.E.T., Tiryakioğlu, I., Tatar, O.R.H.A.N., Demirel, M.E.H.M.E.T., ... and Sığırcı, R.: 2019, Determination of the block movements in the eastern section of the Gediz Graben (Turkey) from GNSS measurements. *J. Geodyn.*, 123, 38–48. DOI: 10.1016/j.jog.2018.11.001
- Ren, A., Xu, K. and Shao, Z.: 2022, Establishment and analysis of GPS coordinate time series noise model in GEONET. *J. Navig. Position.*, 10, 2, 141–151. DOI: 10.16547/j.cnki.10-1096.20220218
- Schwarz, G.: 1978, Estimating the dimension of a model. *Ann. Stat.*, 6, 2, 461–464. <http://www.jstor.org/stable/2958889>
- Shu, B., He, Y., Wang, L., Zhang, Q., Li, X., Qu, X., ... and Qu, W.: 2023, Real-time high-precision landslide displacement monitoring based on a GNSS CORS network. *Measurement*, 217, 113056. DOI: 10.1016/j.measurement.2023.113056
- Springer, A., Karegar, M. A., Kusche, J., Keune, J., Kurtz, W. and Kollet, S.: 2019, Evidence of daily hydrological loading in GPS time series over Europe. *J. Geod.*, 93, 10, 2145–2153. DOI: 10.1007/s00190-019-01295-1
- Steinbock, J., Weissenbrunner, A., Juling, M., Lederer, T. and Thamsen, P.U.: 2016, Uncertainty evaluation for velocity–area methods. *Flow Meas. Instrum.*, 48, 51–56. DOI: 10.1016/j.flowmeasinst.2015.09.007
- Sun, X., Lu, T. and Wang, Z.: 2024, Comparative analysis of different deep learning algorithms for the prediction of marine environmental parameters based on CMEMS products. *Acta Geodyn. Geomater*, 21, 343–363. DOI: 10.13168/AGG.2024.0028
- Sun, X., Lu, T., Hu, S., Huang, J., He, X., Montillet, J.P., ... and Huang, Z.: 2023, The relationship of time span and missing data on the noise model estimation of GNSS time series. *Remote Sens.*, 15, 14, 3572. DOI: 10.3390/rs15143572
- Sun, X., Lu, T., He, X. and Huang, J.: 2024, GNSS time series noise characteristics and environmental loading correction considering RMLE algorithm. *J. Navig. Position.*, 12, 1, 21–27. DOI: 10.16547/j.cnki.10-1096.20240103
- Wang, L., Wu, Q., Wu, F. and He, X.: 2022, Noise content assessment in GNSS coordinate time-series with autoregressive and heteroscedastic random errors. *Geophys. J. Int.*, 231, 2, 856–876. DOI: 10.1093/gji/ggac228
- Wang, W., Zhao, B., Wang, Q. and Yang, S.: 2012, Noise analysis of continuous GPS coordinate time series for CMONOC. *Adv. Space Res.*, 49, 5, 943–956. DOI: 10.1016/j.asr.2011.11.032
- Wang, X., Cheng, Y., Wu, S. and Zhang, K.: 2016, An effective toolkit for the interpolation and gross error detection of GPS time series. *Surv. Rev.*, 48, 348, 202–211. DOI: 10.1179/1752270615Y.0000000023
- Wang, Z., He, X.: 2025, COA–VMPE–WD: A Novel Dual-denoising method for GPS time series based on permutation entropy constraint. *Appl. Sci.*, 15, 19, 10418. DOI: 10.3390/app151910418
- Williams, S.D.P.: 2003, The effect of coloured noise on the uncertainties of rates estimated from geodetic time series. *J. Geod.*, 76, 9, 483–494. DOI: 10.1007/s00190-002-0283-4
- Yu, L., Cao, H., Lian, J., Li, Y., Fan, L., Liu, H. and Liu, Y.: 2025, GNSS-PPP for dynamic deformation monitoring of large-scale engineering structures and a case study. *J. Civ. Struct. Health Monit.*, 1–15. DOI: 10.1007/s13349-025-00945-7
- Zhang, J., Bock, Y., Johnson, H., Fang, P., Williams, S., Genrich, J., ... and Behr, J.: 1997, Southern California Permanent GPS Geodetic Array: Error analysis of daily position estimates and site velocities. *J. Geophys. Res., Solid Earth*, 102, B8, 18035–18055. DOI: 10.1029/97JB01380

- Zhou, D., Liu, Y., Feng, Y., Zhang, H., Fu, Y., Liu, Y. and Tang, Q.: 2022, Absolute sea level changes along the coast of China from tide gauges, GNSS, and satellite altimetry. *J. Geophys. Res., Oceans*, 127, 9, e2022JC018994. DOI: 10.1029/2022JC018994
- Zhou, Y., He, X., Montillet, J.P., Wang, S., Hu, S., Sun, X., ... and Ma, X.: 2025, An improved ICEEMDAN-MPA-GRU model for GNSS height time series prediction with weighted quality evaluation index. *GPS Solut.*, 29, 3, 113.
DOI: 10.1007/s10291-025-01867-z
- Zhu, H., Chen, K., Hu, S., Liu, J., Shi, H., Wei, G., Chai, H., Li, J. and Wang, T.: 2023, Using the global navigation satellite system and precipitation data to establish the propagation characteristics of meteorological and hydrological drought in Yunnan, China. *Water Resour. Res.*, 59, e2022WR033126.
DOI: 10.1029/2022WR033126